Cellular Location and Expression of Na+, K+-ATPase α Subunits Affect the Anti-Proliferative Activity of Oleandrin

Peiying Yang[1,2], **Carrie Cartwright**[1], **Ekem Efuet**[1], **Stanley R. Hamilton**[3], **Ignacio Ivan Wistuba**[3], **David Menter**[2], **Crandell Addington**[4], **Imad Shureiqi**[5,6], and **Robert A. Newman**[7,*]

[1]Department of General Oncology, The University of Texas, M. D. Anderson Cancer Center, Houston, Texas

[2]Department of Cancer Biology, The University of Texas, M. D. Anderson Cancer Center, Houston, Texas

[3]Department of Pathology, The University of Texas, M. D. Anderson Cancer Center, Houston, Texas

[4]Phoenix Biotechnology, Inc., San Antonio, Texas

[5]Department of Clinical Cancer Prevention, The University of Texas, M. D. Anderson Cancer Center, Houston, Texas

[6]Department of Gastrointestinal Medical Oncology, The University of Texas, M. D. Anderson Cancer Center, Houston, Texas

[7]Department of Experimental Therapeutics, The University of Texas, M. D. Anderson Cancer Center, Houston, Texas

Abstract

The purpose of this study was to investigate whether intracellular distribution of Na+, K+-ATPase α3 subunit, a receptor for cardiac glycosides including oleandrin, is differentially altered in cancer versus normal cells and whether this altered distribution can be therapeutically targeted to inhibit cancer cell survival. The cellular distribution of Na+, K+-ATPase α3 isoform was investigated in paired normal and cancerous mucosa biopsy samples from patients with lung and colorectal cancers by immunohistochemical staining. The effects of oleandrin on α3 subunit intracellular distribution, cell death, proliferation, and EKR phosphorylation were examined in differentiated and undifferentiated human colon cancer CaCO-2 cells. While Na+, K+-ATPase α3 isoform was predominantly located near the cytoplasmic membrane in normal human colon and lung epithelia, the expression of this subunit in their paired cancer epithelia was shifted to a peri-nuclear position in both a qualitative and quantitative manner. Similarly, distribution of α3 isoform was also shifted from a cytoplasmic membrane location in differentiated human colon cancer CaCO-2 cells

*Correspondence to: Department of Experimental Therapeutics, The University of Texas MD Anderson Cancer Center, 112 Whale Rock Lane, Surry, ME 04684..

Additional supporting information may be found in the online version of this article.

to a peri-nuclear position in undifferentiated CaCO-2 cells. Intriguingly, oleandrin exerted threefold stronger anti-proliferative activity in undifferentiated CaCO-2 cells (IC50, 8.25 nM) than in differentiated CaCO-2 cells (IC50, >25 nM). Oleandrin (10 to 20 nM) caused an autophagic cell death and altered ERK phosphorylation in undifferentiated but not in differentiated CaCO-2 cells. These data demonstrate that the intracellular location of Na^+, K^+-ATPase $\alpha 3$ isoform is altered in human cancer versus normal cells. These changes in $\alpha 3$ cellular location and abundance may indicate a potential target of opportunity for cancer therapy.

Keywords

cardiac glycoside; Na; K-ATPase $\alpha 3$ isoform; colon tissues; CaCO-2 cells; oleandrin

BACKGROUND

Cardiac glycosides are a class of compounds traditionally used to treat congestive heart failure whose effectiveness relies on their ability to increase myocardial contractile force [1]. Oleandrin is a lipid soluble cardiac glycoside derived from *Nerium oleander* that has been used for many years in Russia and China for this purpose. In addition to its use for treatment of heart failure, preclinical, and retrospective patient data suggest that certain cardiac glycosides, (e.g., digoxin, digitoxin, ouabain, and oleandrin), may also reduce the growth of various malignant diseases such as breast, lung, prostate, pancreatic cancers, and leukemia [2–7]. Recent work from our laboratory and others showed that these compounds induce selective cell death in certain human but neither murine tumor cells [8,9] or normal human cells [10]. Oleandrin inhibits proliferation of human pancreatic cancer cells through induction of autophagic cell death while inducing apoptosis in prostate cancer cells due to an increase in intracellular Ca^{2+} via inhibition of Na^+, K^+-ATPase [5,11]. Other investigators have reported that cardiac glycoside drugs, such as digitoxin and oleandrin, inhibit constitutive hypersecretion of the NF-κB-dependent pro-inflammatory cytokine IL-8 from cystic fibrosis (CF) lung epithelial cells [12] and suppress the TNF-α/NF-κB signaling pathway by blocking TNF-α-dependent TNFR1/TRADD complex formation [13]. Hence, there are many reported mechanisms that appear to be involved in oleandrin-mediated inhibition of proliferation of human tumor cells.

Oleandrin, as well as other cardiac glycosides, has been shown to bind to and inhibit the activity of Na^+, K^+-ATPase [14]. In line with this, a number of studies including our own suggest that the strong sensitivity of human cancer cell lines to cardiac glycosides is most likely related to the relative expression of particular Na^+, K^+-ATPase subunits in these cells as opposed to nonmalignant human cells or those derived from rodent species [15–17]. In support of this, a recent study has demonstrated that oleandrin binds to the plasma membrane of human lymphoma U937 cells but does not bind to murine NIH3T3 cells [9]. Most recently, we have shown that the selective effect of oleandrin on growth inhibition of human and mouse pancreatic cancer cells was associated with differential expression of the various Na^+, K^+-ATPase α isoforms, especially $\alpha 3$ [17]. Additionally, Lin et al. reported that oleandrin and ouabain induced apoptosis in human melanoma BRO cells while there was no evidence of cell death observed in mouse melanoma B16 cells even at concentrations

1,000-fold higher than that used for BRO cells. Partially purified Na$^+$, K$^+$-ATPase from human BRO cells was inhibited at a concentration that was 1,000-fold less than that which was required to inhibit mouse B16 enzyme to the same extent. They also demonstrated that human BRO cells were found to express both the sensitive α3 isoform and the less sensitive α-1 isoform of Na$^+$, K$^+$-ATPase while mouse B16 cells expressed only the α-1 iso-form. These data again suggest that differential expression of Na$^+$, K$^+$-ATPase isoforms in BRO and B16 cells as well as cellular drug uptake may be important determinants of tumor cell sensitivity to oleandrin [15].

It is well established that Na$^+$, K$^+$-ATPase enzyme serves as a pharmacologic receptor for cardiac glyco-sides. Recent findings suggest that, in addition to acting as an ion pump, Na$^+$, K$^+$-ATPase is also engaged in the assembly of signal transduction complexes that transmit signals to different intracellular compartments and in tight junction regulation of epithelial cells [18,19]. Thus, the α-3 isoform of Na, K-ATPase may represent an important new target in anticancer therapy [18,20,21].

Structurally, Na$^+$, K$^+$-ATPase exists as a heterodimer that contains catalytic α-subunits and glycosylated β-subunits. The α-subunit has binding sites for ATP, Na$^+$, K$^+$, and cardiac glycosides. Four different a isoforms (α1, α2, α3, and α4) and three different β isoforms (β1, β2, and β3) have been identified in mammalian cells. The expression of a isoforms is tissue-type specific and varies among rodent and human tissues [22]. Variation in the expression of these isoforms occurs in human cancers (e.g., renal, lung, hepatocellular, and colon) and contrasts with corresponding normal tissues [23–26]. The binding affinity of cardiac glycosides varies depending on the a isoforms present particularly in rodent tissues; the α1 binding affinity is low while the α2 and α3 isoforms bind cardiac glycosides with an affinity as much as 100-fold higher [27,28].

In contrast to our understanding of tissue distribution and cardiac glycoside binding capacity of Na$^+$, K$^+$-ATPase isoforms, knowledge of the cellular distribution of these isoforms under physiological and pathological conditions, such as cancer, is limited. The fact that Na$^+$, K$^+$-ATPase is a transmembrane protein suggests that this enzyme is predominantly present in the plasma membrane [29]. Adrenergic agonists increase the pump's affinity for Na$^+$ and recruit sodium pump subunits to the basolateral plasma membrane from intra-cellular endosomal compartments of lung alveolar epithelial cells [30,31]. The relative distribution of the Na$^+$, K$^+$-ATPase subunits, especially α3, in malignant disease has only recently been reported [32]. How the presence and intracellular distribution of this particular subunit of Na$^+$, K$^+$-ATPase affects the anticancer activity of cardiac glycosides has yet to be determined.

The purpose of the present study was to determine the difference in distribution of Na$^+$, K^{+-}ATPase α3 subunits in human malignant and paired normal colon and lung tissues derived from patient samples. In addition, the change in distribution of Na$^+$, K$^+$-ATPase α3 subunit in malignant (undifferentiated) and well-differentiated human colon cells in culture was explored along with the relative difference in sensitivity this makes when cells are exposed to oleandrin. It was found that the α3 subunit of Na$^+$, K$^+$-ATPase was primarily located in the cytoplasmic membrane in human normal colon or lung tissue while the location shifts to

a peri-nuclear position in colon and lung tumor tissues. The transformation of human colon cancer CaCO-2 cells to those which are well-differentiated reversed the shift back from peri-nuclear to a cytoplasmic position. The lower sensitivity of differentiated as opposed to undifferentiated cells due to oleandrin was also observed.

MATERIALS AND METHODS

Human Tissue Section

Surgically resected specimens of normal and malignant colorectal and lung tissues were obtained from patients at The University of Texas M. D. Anderson Cancer Center through the Tissue Procurement and Banking Facility. Samples were procured from both the tumor area and adjacent normal-appearing mucosa. The UT/MD Anderson Cancer Center Institutional Review Board approved these studies.

Cell Lines

Human colorectal cancer CaCO-2 cells were kindly provided by Dr. Imad Shureiqi at the University of Texas M. D. Anderson Cancer Center. Human colorectal cancer HT29 cells were purchased from American Type Culture Collection (Manassas, VA). Cells were maintained in MEM medium supplemented with 10% fetal bovine serum (Invitrogen, Carlsbad, CA), 50 IU/ml penicillin and 50 μg/ml streptomycin, and 2 mM L-glutamine from GIBCO (Grand Island, NY) at 37°C in 5% CO_2. To induce spontaneous differentiation, CaCO-2 cells (1×10^5) were plated and grown for 14 d without passing the cells. Media was replaced every other day. The differentiation of HT-29 cells was accomplished by treatment with sodium butyrate (2.5 mM) for 72 h.

Antibodies and Reagents

Oleandrin was purchased from ChromaDex (Irvine, CA). DAPI (4′-6-diamidino-2-phenylindole) was obtained from Molecular Probes-Invitrogen Corporation. Anti-Na$^+$, K$^+$-ATPase α3 and anti–β-actin antibodies were purchased from Sigma Chemical Co. (St. Louis, MO). Anti-ERK, anti-phosphorylated ERK (Thr^{202}/Tyr^{204}) and Pan-Cadherin antibodies were purchased from Santa Cruz Biotechnology (Santa Cruz, CA). Anti-LC3 antibody was obtained from Cell Signaling (Billerica, MA).

Cell Proliferation

Undifferentiated wild-type and well-differentiated CaCO-2 cells were treated with a range of concentrations of oleandrin (0.2–25 nM). After 48 h, cells were labeled with BrdU and relative cell proliferation was determined with a BrdU Cell Proliferation Kit according to manufacturer's instruction (Calbiochem-NovaBiochem Corp., San Diego, CA).

Cell Viability and DNA Staining

Cell viability was performed using the vital dye calcien AM (CAM) ester (Life Technologies Corp., Carlsbad, CA) according the method published previously [33]. CAM ester is plasma membrane permeable and non-fluorenscencet before activation by nonspecific esterase within viable cells. The cleavage product CAM emits green

fluorsecence that is retained by viable cells. When plasma membrane integrity is disrupted in the latter stages of cell death, cells fail to effectively retain CAM. Cells were plated in 96-cell plates and incubated with oleandrin (5–20 nM) for 24 h. Cells were then stained with with CAM ester (1 μM), DAPI (300 nM), and Mitrotracker dye (100 nM) in HEPEs-buffered saline for 15 min at 25°C. DNA dye uptake and cellular staining were assessed by fluorescence microscopy using an IPlabs image-analysis system (Scanalytic, Inc., Fairfax, VA) on an IX70 inverted microscope (Olympus, Melville, NY). Fluorescence was quantitated using a Biolumin 960 plate reader.

Isolation of Cytosolic and Membrane Proteins

Cells (about 90% confluent) were washed with PBS followed with addition of 1 ml of NB buffer and were then scrapped. After incubation on ice for 10 min, cells were transferred to a Dounce homogenizer and homogenized using 50 strokes on ice; the contents were then centrifuged at 800g for 5min. The supernatant was further centrifuged (8,000g for 10 min). The supernatant was then collected and subjected to further centrifugation at 100,000g for 30 min. The cytosolic protein fraction was collected as supernatant. The pellet was air dried and resus-pended in 50 μl of 9 M urea as membrane fraction protein. Aliquots of the total cell extract, cytosolic and membrane proteins were used to determine the protein concentrations and subjected to determination of α3 and Pan-Cadherin protein by Western blotting.

Immunoblotting Analysis

Undifferentiated and differentiated CaCO-2 cells were treated in serum-free conditions with 10 and 20 nM oleandrin for 24 h. Cells were then washed with cold phosphate-buffered saline (PBS) and scraped free using lysis buffer containing 20 mM MOPS, 2 mM EGTA, 5 mM EDTA, 30 mM NaF, 40 mM b-glycerophosphate, 20 mM sodium pyruvate, 0.5% triton X-100, and 1 mM sodium orthovanadate with 1× protease inhibitor cocktail (Sigma, Inc., St. Louis, MO). Lysates were then subjected to sonication for 3 min while on ice, incubated for 10 min and then centrifuged (14,000 rpm) for 10 min at 4°C. Protein levels were quantified via the BioRad Dc protein assay (BioRad, Inc., Hercules, CA). Equal levels of protein (50 μg) were fractionated on precast gels (BioRad, Inc.) and then transferred on polyvinylidene diflouride membranes. Following a 1- to 2-h incubation in 5% nonfat dry milk blocking buffer prepared in tris-buffered saline with 0.1% Tween 20 (TBS-T), membranes were probed with ERK, pERK, and LC-3 protein primary antibodies diluted 1:2,000 in blocking buffer. For analysis of α3 and Pan-Cadherin proteins, membranes were probed with α3 (1:1,000) and Pan-Cadherin (1:200) protein primary antibodies diluted in blocking buffer. Protein bands were visualized via chemiluminesence, using the ECL+ detection kit and hyper-film (Amersham Biosciences, Piscataway, NJ). Equal loading of samples was illustrated by Western blotting for β-actin content.

Transmission Electron Microscopy

As oleandrin is known to induce noticeable auto-phagic cell death in human Panc-1 cells [11], we determined whether oleandrin had an equal ability to produce autophagic cell death in undifferentiated and differentiated CaCO-2 cells. To detect the induction of autophagy

morphologically in oleandrin-treated cells, cellular structural alteration was examined by transmission electron microscopy (TEM). Undifferentiated CaCO-2 cells were grown on glass coverslips for 24 h prior to treatment with 20 nM oleandrin. Cells were then washed with cold PBS and prepared for electron microscopy. This included fixation with a solution of 3% glutaraldehde plus 2% paraformaldehyde in 0.1 M cacodylate buffer, pH 7.3 for 1 h. Samples were then postfixed in 1% OsO_4 in the same buffer for 1 h and subsequently subjected to electron microscopic analysis. Representative areas were chosen for ultra thin sectioning and viewed with a JEM 1010 transmission electron microscope (JEOL, Peabody, MA) at an accelerating voltage of 80 kV. Digital images were obtained with an AMT imaging system (Advanced Microscopy Techniques, Danvers, MA).

Immunofluorescence Analysis

Undifferentiated or differentiated CaCO-2 cells were established as monolayers on laminin-coated coverslips to perform immunofluorescence studies. Cells were treated with 20 nM oleandrin for 24 h, then fixed in 1% paraformaldehyde prior to processing for immunofluorescence studies. Coverslips were immunolabled with rabbit anti-α3 (Sigma-Aldrich Corp., St. Louis, MO), and Alexa488 labeled secondary antibody (green; Molecular Probes, Eugene, OR) followed by counterstaining to detect DNA with DAPI (blue). Nuclear morphology, DNA dye uptake, and cellular staining were assessed by fluorescence using an Olympus IX-70 inverted microscope. Image acquisition was achieved using a Quantix charged coupled device camera and IP Labs software (Scanalytics, Inc., Rockville, MD) on a Macintosh computer (Apple, Cupertino, CA).

Immunohistochemical Staining of Human Tissues

Frozen sections from both the tumor area and the normal-appearing mucosa were cut, fixed in acetone, and air dried. At the time of staining, the sections were incubated with 3% hydrogen peroxidase in ethanol for 20 min to inactivate endogenous peroxides. Nonspecific antibody binding sites were blocked using horse serum. Tissue sections were incubated overnight in 1:500—anti-human Na^+, K^+-ATPase polyclonal antibody at 4°C. The next day, the sections were washed and incubated with secondary antibody (mouse IGg, Vector Laboratories, Inc., Burlingame, CA) and then processed similar to what was previously described [34]. Immunohistochemistry (IHC) staining of colorectal cancer samples was scored by a pathologist (S.R.H.) who is highly experienced in colorectal IHC. Staining was uniformly shifted from plasma cell membrane to a cytoplasmic/nuclear distribution in all 31 colorectal cases examined. Lung IHC staining was scored in a bind manner by a pathologist who is highly experienced in lung IHC studies (I.I.W.) in a manner similar to that described previously [35,36]. Briefly, the cytoplasmic expression of the Na^+, K^+-ATPase α-3 subunit was quantified by using a system in which values obtained were the result of multiplying staining intensity scores (0, 1+, 2+, with 3+) by the percentage of stained epithelial cells (0–100%).

RESULTS

Differential Location of the α3 Subunit of Na⁺, K⁺-ATPase in Normal and Malignant Human Lung and Colon Tissues

It has been reported that α3 subunits are primarily localized in the plasma membrane of neurons [37], however, the relative location and distribution of α-3 in tumor tissues has yet to be determined. Immunohistochemistry staining of frozen human normal colon and tumor tissues showed that the Na^+, K^+-ATPase α3 subunit was in or near the plasma membrane of normal colon epithelial cells in 31 of 31 examined cases. In contrast, α3 subunit-distribution in tumor tissue was shifted to a cytoplasmic/nuclear distribution in 31 of 31 examined cases (Figure 1A). A similar differential distribution was also observed in human normal and tumor lung tissues. As shown in Figure 1B, quantitative analysis of the immnuohistochemical staining of Na^+, K^+-ATPase α3 protein clearly suggested that levels of α3 subunits in the cytoplasm were almost twofold higher than that in the nuclear location in normal human lung tissues. In line with the α3 staining of normal colon and cancer tissues, the extent of α3 subunit localized in or near nuclei was about threefold higher than that in the cytoplasm of human lung tumor tissues (Figure 1 B).

Alteration of Location of α3 in Undifferentiated Colon Cancer CaCO-2 and HT-29 Cells and Differentiated CaCO-2 and HT-29 Cells

In order to determine changes in relative α3 intracellular location with respect to phenotypical changes of epithelial cells, we examined the location of this subunit in undifferentiated human colon cancer CaCO-2 and HT-29 cells and the spontaneous differentiated phenotype of CaCO-2 cells and differentiated HT-29 induced by sodium butyrate. In undifferentiated cells, the α3 subunits were distributed in both cytosolic and peri-nuclear positions as evidenced by the intensity of green fluorescence being stronger in the peri-nuclear position [Figure 2A(a) and B(a)]. Intriguingly, the green fluorescence staining of the α3 protein was shifted to a membrane position in well-differentiated CaCO-2 and HT-29 cells [Figure 2A(b) and B(b)]. To further confirm the intracellular distribution of α3 subunits in differentiated and undifferentiated human colon cancer cells, cytosolic and membrane proteins were isolated in undifferentiated and differentiated HT-29 cells and expression of α3 was determined by Western blot analysis. While the total amount of α3 expression in both undifferentiated and differentiated HT-29 cells did not appear to be different, the level of membranous α3 was relatively higher in differentiated HT-29 cells compared to that of undifferentiated HT-29 cells (Supplementary Figure S1).

Differential Sensitivity of Undifferentiated and Differentiated CaCO-2 to Oleandrin Treatment

When treated with a series of concentrations of oleandrin (0.2–25 nM), the undifferentiated CaCO-2 cells were sensitive as evidenced by an IC_{50} of 8.25 nM. In contrast, a maximum growth inhibition of only 20% was reached in differentiated CaCO-2 cells even though they were treated with oleandrin concentrations as high as 25 nM (Figure 3). These findings demonstrate that wild-type CaCO-2 cells are more sensitive to oleandrin than are differentiated CaCO-2 cells and further suggest that the change in sensitivity to this cardiac glycoside may be associated with the shift in intracellular location of α3.

To further confirm the differential anti-proliferative activity of oleandrin in undifferentiated and differentiated CaCO-2 cells, we examined ultrastructural changes in these cells. As shown in Figure 4A, oleandrin (20 nM) treated undifferentiated CaCO-2 cells exhibited a large number of vacuoles (Figure 4A, c) and condensed mitochondria with typical autophagosome bodies (Figure 4A, d) compared to that of vehicle treated undifferentiated CaCO-2 cells (Figure 4A, a and b), respectively. In contrast, oleandrin failed to induce autophagic cell death in differentiated CaCO-2 cells. In fact, the ultrastructure of both control and oleandrin treated differentiated CaCO-2 cells was very similar with few vacuoles or autophagosome bodies present (Figure 4B, a–d). The cell viability in oleandrin treated undifferentiated CaCO-2 cells was further tested using DNA uptake dye DAPI and CAM ester which stains viable cells. Cells treated with oleandrin (20 nM) showed a reduced green fluorescence and relatively stronger DNA uptake of DAPI dye compared to control cells, suggesting oleandrin was able to inhibit proliferation of CaCO-2 cells in a concentration dependent manner (Supplementary Figure S2).

Regulation of LC-3 Proteins and ERK Pathways in Undifferentiated and Differentiated CaCO-2 Cells

As long chain 3 (LC-3) protein is a hallmark associated with autophagic cell death, the expression of this particular protein in both undifferentiated and differentiated CaCO-2 cells was examined. Because we reported previously that increased phosphorylation of ERK protein was associated with oleandrin induced autophagic cell death [11], we also examined total ERK and phospho-ERK expression. Interestingly, while the expression of both LC-3 I and II proteins in undifferentiated CaCO-2 cells was increased by oleandrin treatment (Figure 5A), LC3-I protein levels were only slightly increased by a similar concentration of oleandrin in differentiated CaCO-2 cells (Figure 5B). Similarly, oleandrin treatment increased phosphorylation of ERK in a concentration dependent manner in undifferentiated CaCO-2 cells (Figure 5A, a and b). Surprisingly, both expression of total ERK and phosphorylated ERK proteins remained unaltered by oleandrin treatment in differentiated CaCO-2 cells (Figure 5B, a and b). These results again support the notion that elevated LC-3 protein and ERK phosphorylation might be involved in oleandrin induced autophagic cell death in undifferentiated CaCO-2 cells.

DISCUSSION

Our group and others have observed that a wide number of human cancer cell lines are 100-fold or greater more sensitive to oleandrin than are murine tumor cells, normal human epithelial cells, peripheral blood mononuclear cells or neutrophils [8,10,15,17,38]. This differential sensitivity of human and murine cancer cells to oleandrin treatment might be linked to distinct expression of Na^+, K^+-ATPase $\alpha 3$ subunit in these cells. As a seven-membrane transmembrane protein, Na^+, K^+-ATPase is typically reported to be located in the plasma membrane [29]. The apparent differences in observed enzyme location between normal and malignant tissue sections prompted us to determine if the differential binding capability of human cancer cells to oleandrin was associated with a particular distribution of the isoforms of Na^+, K^+-ATPase in normal and malignant cell phenotypes. Given that translocation of membrane proteins sometimes plays an important role in their related

biological function, understanding the location of Na$^+$, K$^+$-ATPase α3 subunit associated with the differential inhibitory effect of oleandrin may be important in further defining the critical role of this enzyme as a novel anticancer drug target.

The data in the present study demonstrate that normal as opposed to tumor colon and lung tissues exhibited distinctly different distributions of the Na$^+$, K$^+$-ATPase α3 subunit by immunohistochemical staining. The α3 subunit was predominantly located in the cytoplasmic membrane in both normal colon and lung tissues, whereas distribution of this subunit was shifted to a predominantly peri-nuclear position in tumor tissues. Intriguingly, the spontaneous phenotypic change of human colon cancer CaCO-2 cells from undifferentiated to differentiated condition to resemble normal intestinal epithelial cells [39] reversed the position of Na$^+$, K$^+$-ATPase α3 subunit from the peri-nuclear position to the cytoplasmic membrane. These data suggest that pheno-typical changes of cells or pathological alteration of tissues may correlate with the location of this enzyme subunit which, in turn, suggests a direct relation to the function of the enzyme. To explore this, the effect of oleandrin on proliferation of undifferentiated and differentiated CaCO-2 cells was examined. While proliferation of undifferentiated CaCO-2 cells was inhibited by as much as 70% when treated with 25 nM oleandrin, <20% inhibition of cell proliferation was observed in well-differentiated CaCO-2 cells. In line with this, oleandrin-induced noticeable autophagic cell death in undifferentiated CaCO-2 cells but only small auto-phagosome bodies were observed in oleandrin treated differentiated CaCO-2 cells. The difference in response of undifferentiated and differentiated CaCO-2 cells to oleandrin treatment was also evidenced by a marked elevation of phospho-Erk in undifferentiated as opposed to differentiated CaCO-2 cells. These results suggest an important role of the cellular location of α3 in anticancer activity of oleandrin in human cancers.

The α subunit is a multispanning membrane protein that catalyzes ion transport and contains binding sites for cations, ATP and cardiac glycosides [27,40]. The four a isoforms of Na$^+$, K$^+$-ATPase, α1, α2, α3, and α4, are each derived from separate genes. One obvious difference amongst the isoforms is in their response to exposure to cardiac glyco-sides. While the Na$^+$, K$^+$-ATPase α1 subunit has been considered as a "housekeeping" isoform due to its ubiquitous cellular presence, the α2 and α3 iso-forms exhibit more distinct patterns of distribution. The α3 subunit is found in high concentrations in neurons of the central nervous system as well as in cardiac muscle tissues while a lower expression of this particular subunit was observed in ovary, cartilage, and bone [37]. In addition, these Na$^+$, K$^+$- ATPase isoforms have been also reported to be differentially distributed in subcellular fractions. For example, α1 is universally distributed in the plasma membrane of rat myocytes, however, the α3 subunit is distributed in the plasma membrane in reticular patterns that parallel the underlying ER [41]. These different subcellular distribution patterns suggest a potential association with the function of these a isoforms due to their differential cardiac glycoside binding affinities. Even though emerging evidence has suggested a role of Na$^+$, K$^+$-ATPase in the development of various cancers, knowledge of the relative subcellular distribution of this particular enzyme and its isoforms in tumor biology is very limited. Mijatovic et al. [42] reported that the α1 isoform was elevated in lung cancer in comparison to that of adjacent normal tissues. While the result of that study does not seem to support the over-expression of α3 in lung tumor tissues compared to that of normal controls,

the subcellular distribution of α3 in human lung normal or tumor tissues was not examined. We report for the first time that the Na$^+$, K$^+$-ATPase α3 isoform is primarily located in the plasma membrane of the normal colon or lung tissues but is altered to a cytosolic peri-nuclear position in colon or lung tumor tissues. The observed changes in subcellular location of α3 in human tissues are also substantiated by the fact that the α3 cellular distribution was altered in human undifferentiated colon cancer CaCO-2 and HT29 cells upon being made to undergo differentiation suggesting that the translocation of Na$^+$, K$^+$-ATPase α3 isoform might be linked to the phenotypical changes of colon or lung tissues. Our finding is in a good agreement with the very recent report by S. A. Rajasekaran who observed that Na$^+$, K$^+$-ATPase α1/β1 was predominantly localized at the plasma membrane of porcine proximal tubule-like kidney LLC-PK1 cells, whereas a distinct intracellular distribution surrounding the nucleus was observed in TGF-β1 treated LLC-PK1 cells [43]. It was suggested that the altered Na$^+$, K$^+$-ATPase location is an early event in the TGF-β1-mediated induction of EMT and is associated with the progression of EMT in cancer and fibrosis [43]. Whether the translocation of Na$^+$, K$^+$-ATPase α3 is essential for the development of the colon or lung tumor certainly deserves further investigation.

CONCLUSION

In summary, we report a change in the location of Na$^+$, K$^+$-ATPase α3 isoform from a cytoplasmic membrane position in normal control tissues to a peri-nuclear position in both human colon and lung tumor tissues. The alteration of the α3 isoform position in normal versus tumor cells was recapitulated in undifferentiated and differentiated human colon CaCO-2 and HT29 cells. Given that a number of investigators have explored the antitumor potential of cardiac glycosides, particularly its relationship to Na$^+$, K$^+$-ATPase, the present data suggest both the relative level of expression of the α3 isoform as well as its cellular distribution play important roles in oleandrin-induced anticancer effects.

Supplementary Material

Refer to Web version on PubMed Central for supplementary material.

ACKNOWLEDGMENTS

Abbreviations

CF	cystic fibrosis
CAM	calcien AM
PBS	phosphate-buffered saline
TEM	transmission electron microscopy
IHC	immunohistochemistry
LC-3	long chain 3

| **ERK** | extracellular signal-related kinase |
| **EMT** | epithelial mesenchymal transition |

REFERENCES

1. Kjeldsen K, Norgaard A, Gheorghiade M. Myocardial Na, K-ATPase: The molecular basis for the hemodynamic effect of digoxin therapy in congestive heart failure. Cardiovasc Res. 2002; 55:710–713. [PubMed: 12176120]

2. Haux J. Digitoxin is a potential anticancer agent for several types of cancer. Med Hypotheses. 1999; 53:543–548. [PubMed: 10687899]

3. Stenkvist B. Is digitalis a therapy for breast carcinoma? Oncol Rep. 1999; 6:493–496. [PubMed: 10203580]

4. Yeh JY, Huang WJ, Kan SF, Wang PS. Inhibitory effects of digitalis on the proliferation of androgen dependent and independent prostate cancer cells. J Urol. 2001; 166:1937–1942. [PubMed: 11586264]

5. McConkey DJ, Lin Y, Nutt LK, Ozel HZ, Newman RA. Cardiac glycosides stimulate Ca^{2+} increases and apoptosis in androgen-independent, metastatic human prostate adenocarcinoma cells. Cancer Res. 2000; 60:3807–3812. [PubMed: 10919654]

6. Turan N, Akgun-Dar K, Kuruca SE, et al. Cytotoxic effects of leaf, stem and root extracts of *Nerium oleander* on leukemia cell lines and role of the p-glycoprotein in this effect. J Exp Ther Oncol. 2006; 6:31–38. [PubMed: 17228522]

7. Frese S, Frese-Schaper M, Andres AC, Miescher D, Zumkehr B, Schmid RA. Cardiac glycosides initiate Apo2L/TRAIL-induced apoptosis in non-small cell lung cancer cells by up-regulation of death receptors 4 and 5. Cancer Res. 2006; 66:5867–5874. [PubMed: 16740726]

8. Pathak S, Multani AS, Narayan S, Kumar V, Newman RA. Anvirzel, an extract of *Nerium oleander*, induces cell death in human but not murine cancer cells. Anticancer Drugs. 2000; 11:455–463. [PubMed: 11001386]

9. Raghavendra PB, Sreenivasan Y, Ramesh GT, Manna SK. Cardiac glycoside induces cell death via FasL by activating calcineurin and NF-AT, but apoptosis initially proceeds through activation of caspases. Apoptosis. 2007; 12:307–318. [PubMed: 17203245]

10. Sreenivasan Y, Raghavendra PB, Manna SK. Oleandrin-mediated expression of Fas potentiates apoptosis in tumor cells. J Clin Immunol. 2006; 26:308–322. [PubMed: 16779680]

11. Newman RA, Kondo Y, Yokoyama T, et al. Autophagic cell death of human pancreatic tumor cells mediated by oleandrin, a lipid-soluble cardiac glycoside. Integr Cancer Ther. 2007; 6:354–364. [PubMed: 18048883]

12. Srivastava M, Eidelman O, Zhang J, et al. Digitoxin mimics gene therapy with CFTR and suppresses hypersecretion of IL-8 from cystic fibrosis lung epithelial cells. Proc Natl Acad Sci USA. 2004; 101:7693–7698. [PubMed: 15136726]

13. Yang Q, Huang W, Jozwik C, et al. Cardiac glycosides inhibit TNF-alpha/NF-kappaB signaling by blocking recruitment of TNF receptor-associated death domain to the TNF receptor. Proc Natl Acad Sci USA. 2005; 102:9631–9636. [PubMed: 15983368]

14. Rose AM, Valdes R Jr. Understanding the sodium pump and its relevance to disease. Clin Chem. 1994; 40:1674–1685. [PubMed: 8070076]

15. Lin Y, Dubinsky WP, Ho DH, Felix E, Newman RA. Determinants of human and mouse melanoma cell sensitivities to oleandrin. J Exp Ther Oncol. 2008; 7:195–205. [PubMed: 19066128]

16. Smith JA, Madden T, Vijjeswarapu M, Newman RA. Inhibition of export of fibroblast growth factor-2 (FGF-2) from the prostate cancer cell lines PC3 and DU145 by Anvirzel and its cardiac glycoside component, oleandrin. Biochem Pharmacol. 2001; 62:469–472. [PubMed: 11448457]

17. Yang P, Menter DG, Cartwright C, et al. Oleandrin-mediated inhibition of human tumor cell proliferation: Importance of Na, -ATPase alpha subunits as drug targets. Mol Cancer Ther. 2009; 8:2319–2328. [PubMed: 19671733]

18. Kaplan JH. A moving new role for the sodium pump in epithelial cells and carcinomas. Sci STKE. 2005; 2005:pe31–pe40. [PubMed: 15972700]

19. Xie Z, Cai T. Na$^+$-K$^+$-ATPase-mediated signal transduction: From protein interaction to cellular function. Mol Interv. 2003; 3:157–168. [PubMed: 14993422]

20. Mijatovic T, Van Quaquebeke E, Delest B, Debeir O, Darro F, Kiss R. Cardiotonic steroids on the road to anti-cancer therapy. Biochim Biophys Acta. 2007; 1776:32–57. [PubMed: 17706876]

21. Newman RA, Yang P, Pawlus AD, Block KI. Cardiac glycosides as novel cancer therapeutic agents. Mol Interv. 2008; 8:36–49. [PubMed: 18332483]

22. Blanco G, Mercer RW. Isozymes of the Na-K-ATPase: Heterogeneity in structure, diversity in function. Am J Physiol. 1998; 275:F633–F650. [PubMed: 9815123]

23. Rajasekaran SA, Ball WJ Jr. Bander NH, Liu H, Pardee JD, Rajasekaran AK. Reduced expression of beta-subunit of Na,K-ATPase in human clear-cell renal cell carcinoma. J Urol. 1999; 162:574–580. [PubMed: 10411090]

24. Avila J, Lecuona E, Morales M, Soriano A, Alonso T, Martin-Vasallo P. Opposite expression pattern of the human Na,K-ATPase beta 1 isoform in stomach and colon adenocarcinomas. Ann N Y Acad Sci. 1997; 834:653–655. [PubMed: 9405883]

25. Espineda C, Seligson DB, James Ball W Jr. et al. Analysis of the Na,K-ATPase alpha- and beta-subunit expression profiles of bladder cancer using tissue microarrays. Cancer. 2003; 97:1859–1868. [PubMed: 12673711]

26. Jung MH, Kim SC, Jeon GA, et al. Identification of differentially expressed genes in normal and tumor human gastric tissue. Genomics. 2000; 69:281–286. [PubMed: 11056045]

27. Blanco G. Na,K-ATPase subunit heterogeneity as a mechanism for tissue-specific ion regulation. Semin Nephrol. 2005; 25:292–303. [PubMed: 16139684]

28. Rajasekaran SA, Barwe SP, Rajasekaran AK. Multiple functions of Na,-ATPase in epithelial cells. Semin Nephrol. 2005; 25:328–334. [PubMed: 16139688]

29. Dunbar LA, Caplan MJ. Ion pumps in polarized cells: Sorting and regulation of the Na+, K+- and H+, K+-ATPases. J Biol Chem. 2001; 276:29617–29620. [PubMed: 11404365]

30. Podevin RA, Parini A. Adrenergic agonists and the Na+-K+-adenosine triphosphatase from rabbit proximal tubules and their basolateral membranes. J Pharmacol Exp Ther. 1989; 250:672–677. [PubMed: 2547943]

31. Saumon G, Basset G, Bouchonnet F, Crone C. Cellular effects of beta-adrenergic and of cAMP stimulation on potassium transport in rat alveolar epithelium. Pflugers Arch. 1989; 414:340–345. [PubMed: 2571117]

32. Benfante R, Antonini RA, Vaccari M, et al. The expression of the human neuronal alpha3 Na+,K+-ATPase subunit gene is regulated by the activity of the Sp1 and NF-Y transcription factors. Biochem J. 2005; 386:63–72. [PubMed: 15462673]

33. Yang P, Chan D, Felix E, et al. Formation and antiproliferative effect of Prostaglandin E(3) from eicosapentaenoic acid in human lung cancer cells. J Lipid Res. 2004; 45:1030–1039. [PubMed: 14993240]

34. Shureiqi I, Wojno KJ, Poore JA, et al. Decreased 13-S-hydroxyoctadecadienoic acid levels and 15-lipoxygenase-1 expression in human colon cancers. Carcinogenesis. 1999; 20:1985–1995. [PubMed: 10506115]

35. Raso MG, Behrens C, Herynk MH, et al. Immunohistochemical expression of estrogen and progesterone receptors identifies a subset of NSCLCs and correlates with EGFR mutation. Clin Cancer Res. 2009; 15:5359–5368. [PubMed: 19706809]

36. Moussalli MJ, Wu Y, Zuo X, et al. Mechanistic contribution of ubiquitous 15-lipoxygenase-1 expression loss in cancer cells to terminal cell differentiation evasion. Cancer Prev Res. 2011; 4:1961–1972.

37. Mobasheri A, Avila J, Cozar-Castellano I, et al. Na+, K+-ATPase isozyme diversity; comparative biochemistry and physiological implications of novel functional interactions. Biosci Rep. 2000; 20:51–91. [PubMed: 10965965]

38. Raghavendra PB, Sreenivasan Y, Manna SK. Oleandrin induces apoptosis in human, but not in murine cells: Dephosphorylation of Akt, expression of FasL, and alteration of membrane fluidity. Mol Immunol. 2007; 44:2292–2302. [PubMed: 17173971]

39. Matsumoto H, Erickson RH, Gum JR, Yoshioka M, Gum E, Kim YS. Biosynthesis of alkaline phosphatase during differentiation of the human colon cancer cell line Caco-2. Gastroenterology. 1990; 98:1199–1207. [PubMed: 2323513]

40. Sweadner KJ. Enzymatic properties of separated isozymes of the Na,K-ATPase. Substrate affinities, kinetic cooperativity, and ion transport stoichiometry. J Biol Chem. 1985; 260:11508–11513. [PubMed: 2995339]

41. Juhaszova M, Blaustein MP. Distinct distribution of different Na$^+$ pump alpha subunit isoforms in plasmalemma. Physiological implications. Ann N Y Acad Sci. 1997; 834:524–536. [PubMed: 9405854]

42. Mijatovic T, Roland I, Van Quaquebeke E, et al. The alpha1 subunit of the sodium pump could represent a novel target to combat non-small cell lung cancers. J Pathol. 2007; 212:170–179. [PubMed: 17471453]

43. Rajasekaran SA, Huynh TP, Wolle DG, et al. Na,K-ATPase subunits as markers for epithelial-mesenchymal transition in cancer and fibrosis. Mol Cancer Ther. 2010; 9:1515–1524. [PubMed: 20501797]
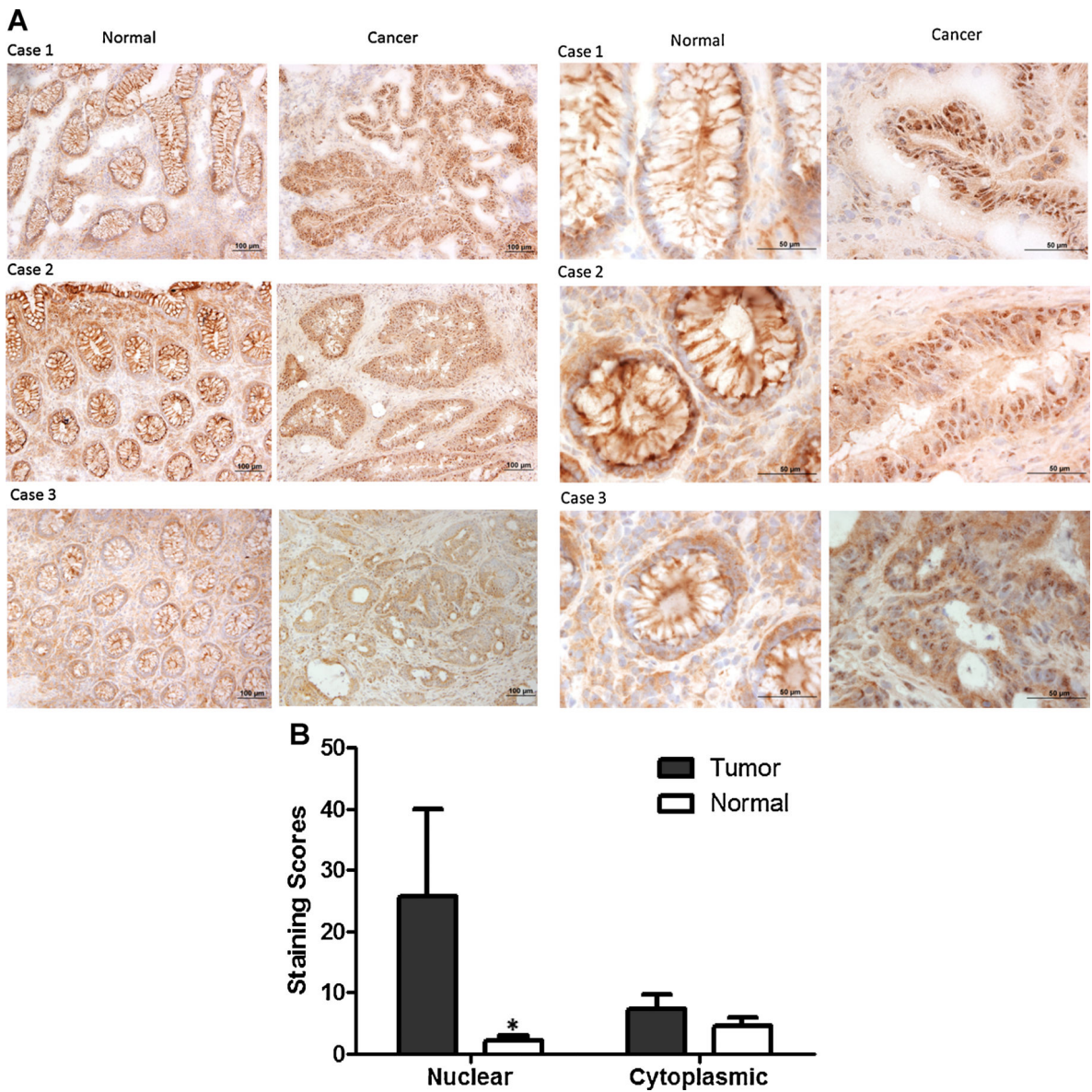
Figure 1.
Differential distribution of Na$^+$, K$^+$-ATPase α-3 isoform in normal and malignant colon or lung cancer tissues by immunohistochemical staining. (A) The distribution of Na$^+$, K$^+$-ATPase α-3 isoform is expressed in or near the plasma membrane in normal tissue sections while the majority of α-3 isoform staining in malignant tissue sections is found in a peri-nuclear position. Left Panel: The IHC staining of Na$^+$, K$^+$-ATPase in normal and tumor colon tissues were taken at a magnification of 100×; Right Panel, the imaging was taken at a magnification of 400×. (B) Na$^+$, K$^+$-ATPase α-3 expression distribution in paired normal and non-small cell lung cancer tissues. Immunohistochemical staining for Na$^+$, K$^+$-ATPase α-3 expression was scored in normal and pair lung tissue samples. Data are presented as mean scores SEM (n ± 20 pair). *$P < 0.05$ tumor versus normal tissue.
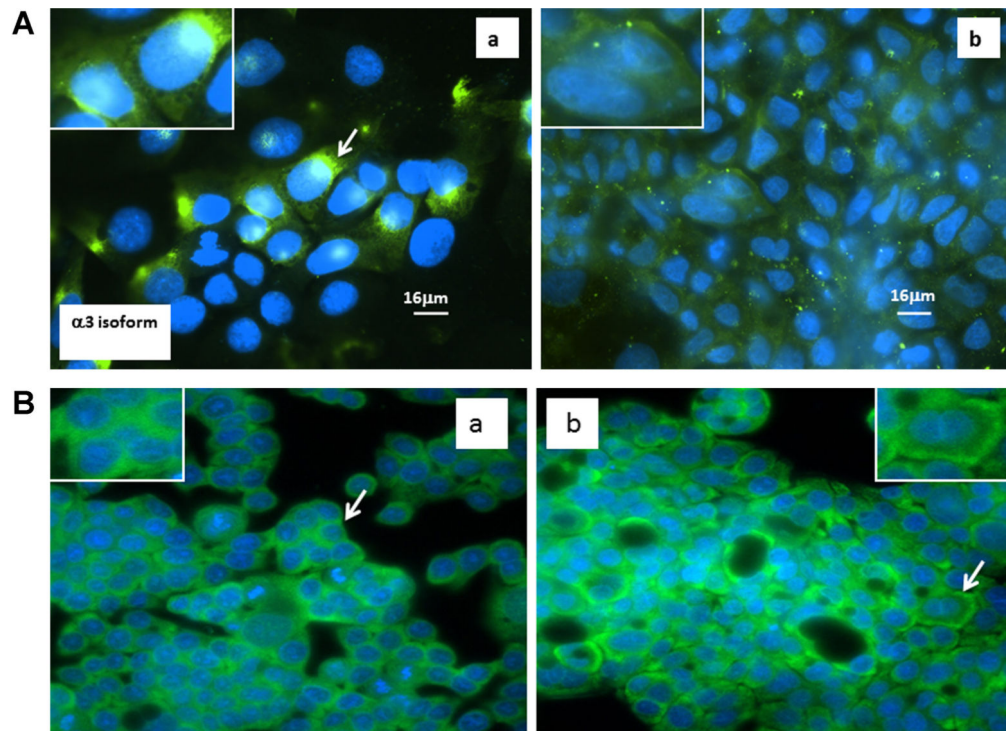
Figure 2.
Distribution of Na$^+$, K$^+$-ATPase α3 isoform in the undifferentiated and differentiated CaCO-2 (A) and HT29 cells (B). *Inserts*, higher magnification of representative cells. Cells were stained for the presence of α-3 (green) and nuclei (blue). A peri-nuclear location of α-3 subunits is evident in A (a) and B (a) while a more diffuse cytoplasmic location of α-3 is shown in A (b) and B (b).
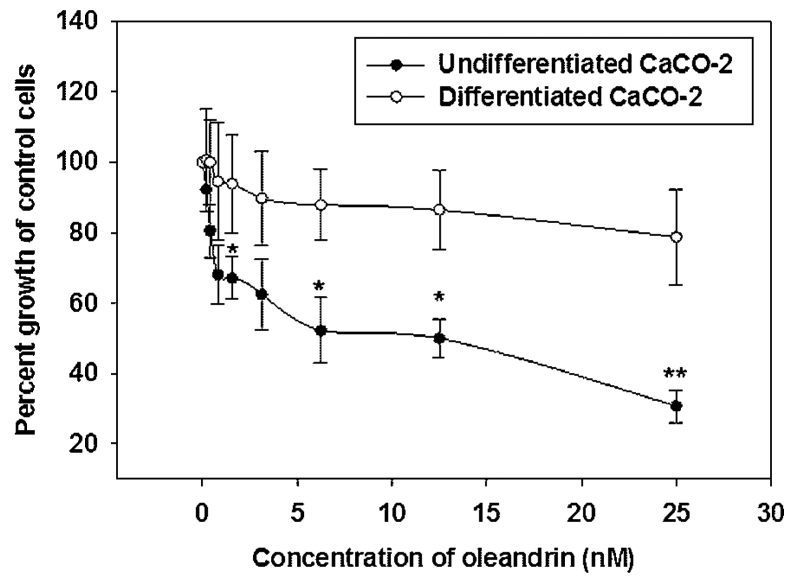
Figure 3.
Anti-proliferative effect of oleandrin in undifferentiated and differentiated CaCO-2 cells.
Cells were treated with a series of concentrations of oleandrin (0.2–25 nM) for 48 h and cell
proliferation was then determined by BrdU staining. Data are presented as mean ± SD of
three separate experiments with *$P < 0.05$, **$P < 0.01$ denoting a significant difference in
response at those individual concentrations of undifferentiated and differentiated CaCO-2
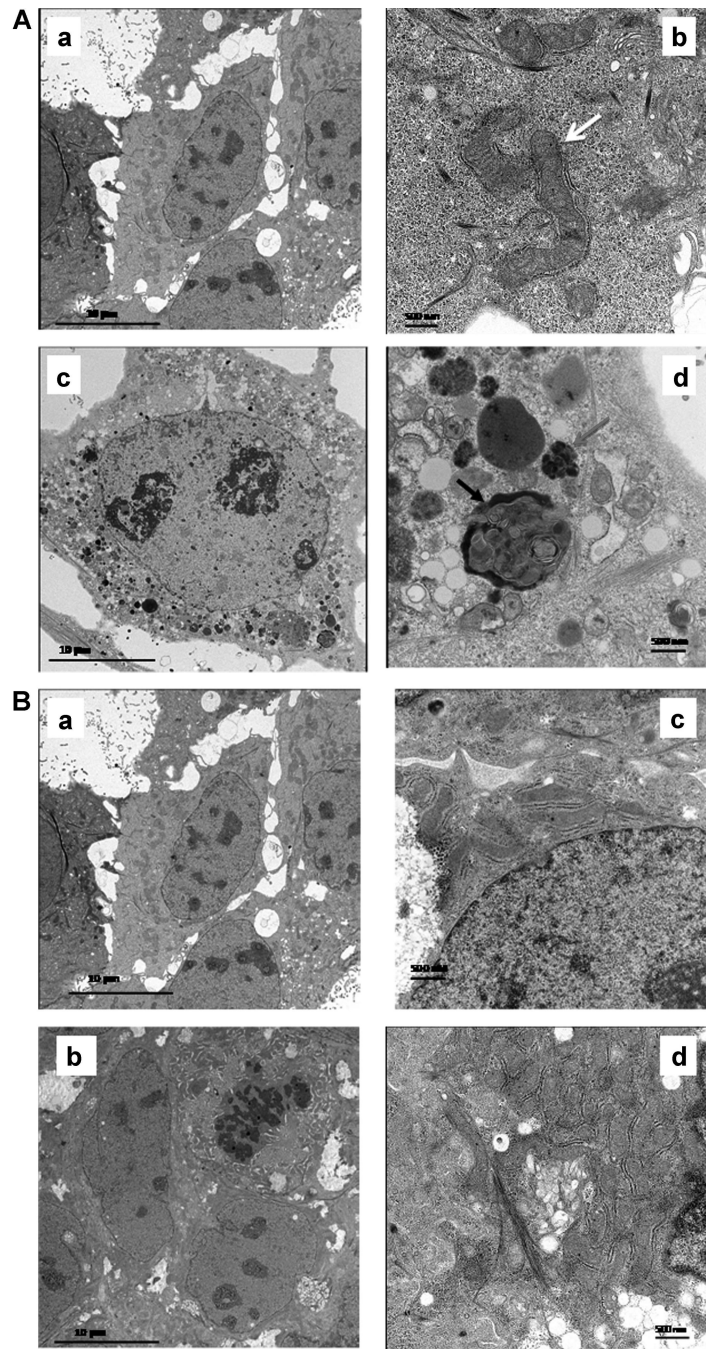cells.

Figure 4.
Autophagic cell death induced by oleandrin in undifferentiated and differentiated CaCO-2 cells. (A) Oleandrin inhibited cell proliferation through induction of autophagic cell death in undifferentiated CaCO-2 cells. The white arrow (b) indicates mitochondria in the control undifferentiated CaCO-2 cells, while the red arrow (d) points to condensed mitochondria in the oleandrin treated undifferentiated CaCO-2 cells. The black arrow ('d') points to an autophagosome formation in the oleandrin treated cells. (a) control CaCO-2 cells (5,000×); (b) control CaCO-2 cells (20,000×); (c) oleandrin (20 nM) treated undifferentiated CaCO-2

cells (5,000×); (d) oleandrin treated undifferentiated CaCO-2 cells (20,000×). (B) Oleandrin treated differentiated CaCO-2 cells showed very limited inhibitory effect on cell proliferation of these particular cells. (a) control differentiated CaCO-2 cells (5,000×); (b) control differentiated CaCO-2 cells (20,000×); (c) oleandrin (20 nM) treated differentiated CaCO-2 cells (5,000×); (d) oleandrin treated differentiated CaCO-2 cells (20,000×). Neither condensed mitochondria nor autophagosome bodies were observed in oleandrin treated differentiated CaCO-2 cells compared to that of vehicle treated differentiated CaCO-2 cells.
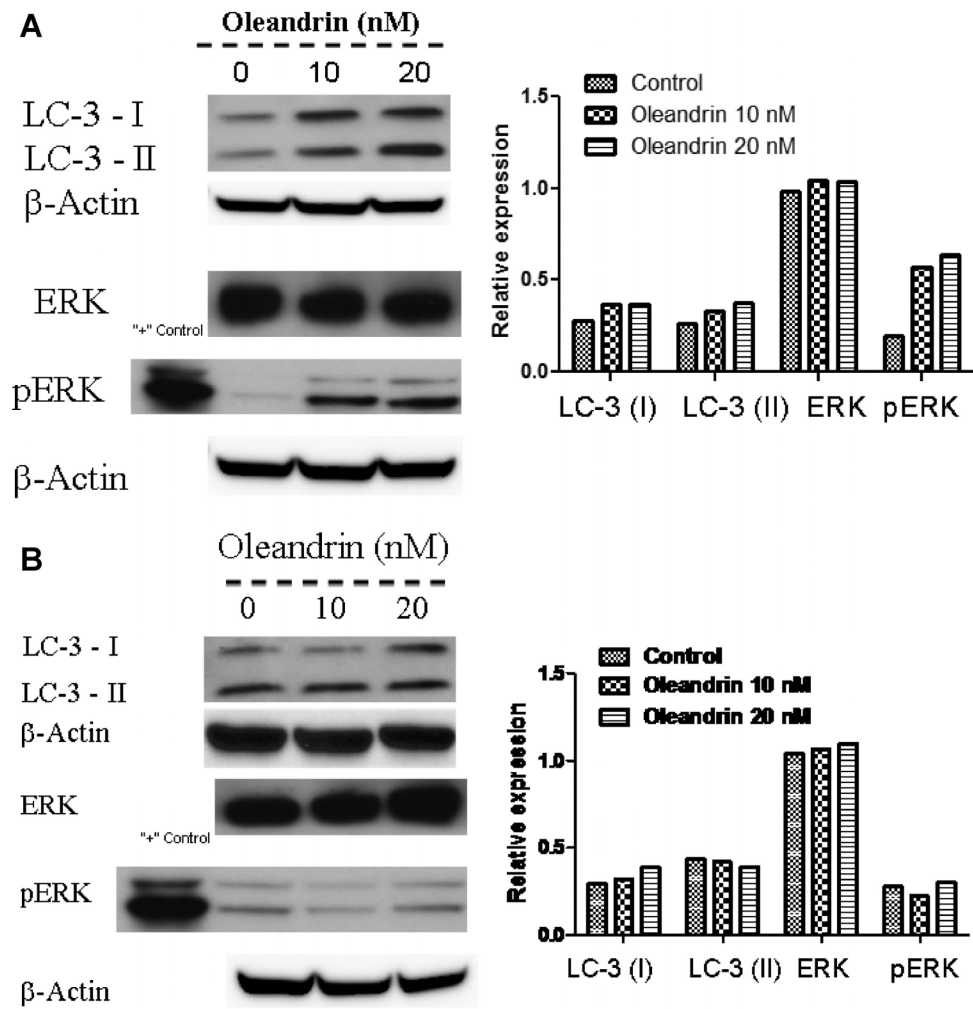
Figure 5.
The effect of oleandrin on expression of long chain 3 (LC-3) protein and ERK as well as pERK in undifferentiated (A) and differentiated (B) CaCO-2 cells. The expression of LC-3 protein (I and II) and pERK was up regulated by oleandrin in undifferentiated but not differentiated CaCO-2 cells. The data are representative of two separate experiments with similar results.